Journal of Industrial and Engineering Chemistry 80 (2019) 551–557

Contents lists available at ScienceDirect

Journal of Industrial and Engineering Chemistry

journal homepage: www.elsevier.com/locate/jiec

Mesoporous carbon/$Li_4Ti_5O_{12}$ nanoflakes composite anode material lithiated to 0.01 V

Chris Yeajoon Bon[a], Phiri Isheunesu[b], Manasi Mwemezi[a], Sangjun Kim[a], Vera Afumaa Afrifah[a], Louis Hamenu[b], Jang Myoun Ko[a,*]

[a] Hanbat National University, Department of Chemical Engineering and Biotechnology, 125 Dongseo-daero, N6-dong, 506-ho, Yuseong-gu, Daejeon 34158, Republic of Korea
[b] Department of Chemistry, School of Physical and Mathematical Sciences, College of Basic and Applied Sciences, University of Ghana, Legon, Ghana

ARTICLE INFO

Article history:
Received 8 March 2019
Received in revised form 5 August 2019
Accepted 12 August 2019
Available online 1 September 2019

Keywords:
Mesoporous carbon
LTO nanoflakes
Composite anode
Lithium ion battery

ABSTRACT

A composite anode material is fabricated from mesoporous carbon and synthesized $Li_4Ti_5O_{12}$ nanoflakes for application in lithium ion batteries. $Li_4Ti_5O_{12}$ is used as a capacity contributing conductive additive because of the change in its electronic structure from insulating to metallic as it undergoes lithiation. Cyclic voltammetry, galvanostatic charge–discharge, and electrochemical impedance spectroscopy are used to analyze the electrochemical properties of the mesporous carbon/$Li_4Ti_5O_{12}$ nanoflakes composite material, and synergistic results have been confirmed. The composite achieves high specific capacity and excellent cyclability with a capacity stabilizing at 300 mA h g^{-1} after 100 cycles at a current density of 175 mA g^{-1} and 200 mA h g^{-1} after 500 more cycles at a high current density of 500 mA g^{-1}. This research shows the applicability of using LTO as a conducting agent with significant capacity contribution as a composite material with anode materials discharged to 0.01 V for high energy storage with fast charge–discharge capability.

Introduction

$Li_4Ti_5O_{12}$ (LTO) is a commonly used anode material well known for its high power capability and long cycle life [1]. LTO is known as a "zero-strain" insertion material which means that there is minimal lattice strain (0.2%) during lithium intercalation and deintercalation [2,3]. This means there is less physical stress on the material allowing it to charge and discharge quickly and last for many cycles. Another reason for LTO's high power capability is that its operating voltage (≈1.5 V) is higher than the potential at which organic electrolytes undergo reduction (<0.7 V) which forms the solid electrolyte interphase (SEI) layer on the anode [4]. Because the SEI layer for LTO anodes is negligible, there is nothing hindering lithium ions from the electrolyte to the electrode surface.

However, graphite anodes remain the standard for lithium ion batteries because it has much higher energy density than LTO which is limited due to high working potental of LTO as well as its low theoretical specific capacity (175 mA h g^{-1}). Consequently, a lot of research has been done in order to increase the energy density of LTO. One possibility is to charge the cell below 1 V inducing another phase change from $Li_7Ti_5O_{12}$ to $Li_9Ti_5O_{12}$, which will lower its working potential as well as increase its specific capacity to 220 mA h g^{-1} [5,6]. This is not commonly done because charging below 1 V results in SEI formation which increases cell resistance and decreases rate capability. However, this can be desirable because of a change in LTO's electronic structure as it is lithiated from $Li_4Ti_5O_{12}$ to $Li_7Ti_5O_{12}$. Ouyang et al. has shown that the conductive nature of LTO changes from insulating to metallic as it undergoes lithiation through calculated density of states [7]. Thus, LTO can be used as a conducting agent while contributing significant capacity to an electrode material in its lithiated ($Li_{7+}Ti_5O_{12}$) state.

The purpose of this research is to fabricate a mesoporous carbon (MC)/LTO nanoflake (LTO-NF) composite electrode and test its electrochemical performance to determine the effect of LTO-NF used in a composite. Carbon is commonly used in composite electrode materials due to its excellent electrochemical properties such as high capacity and conductivity [8–12]. The expected result would be that the capacity of the MC/LTO-NF composite would simply be an average of the two materials,

* Corresponding author.
E-mail address: jmko@hanbat.ac.kr (J.M. Ko).

https://doi.org/10.1016/j.jiec.2019.08.026
1226-086X/

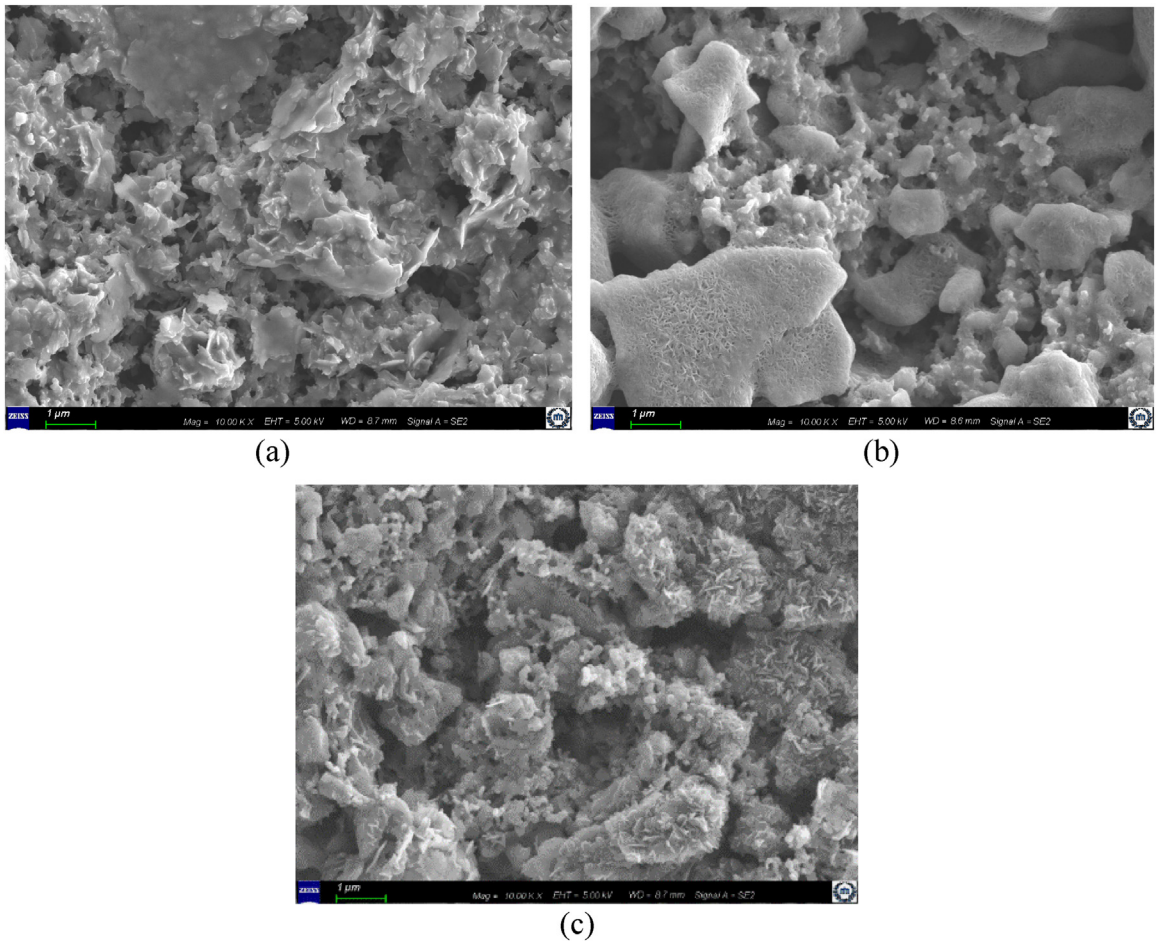

Fig. 1. SEM images of the electrode surfaces at a magnification of 10,000× after 600 cycles for (a) LTO-NF, (b) MC, and (c) MC/LTO-NF.

however our results show that the composite exhibits higher capacity than bare MC at all current densities. This shows a synergistic relationship between MC and LTO-NF, which can be explained by the metallic nature of LTO which has the ability to aid in conduction under 1 V which improves charge transfer kinetics in the electrode by creating pathways facilitating electron movement through MC as well as contributing its own capacity. LTO-NF also has properties such as smaller grain size, higher grain density made up of rutile TiO_2, and increased oxygen deficiencies, which help to give superior electrochemical performance compared to bare LTO, and this has been explained in more detail in previous research [13–15].

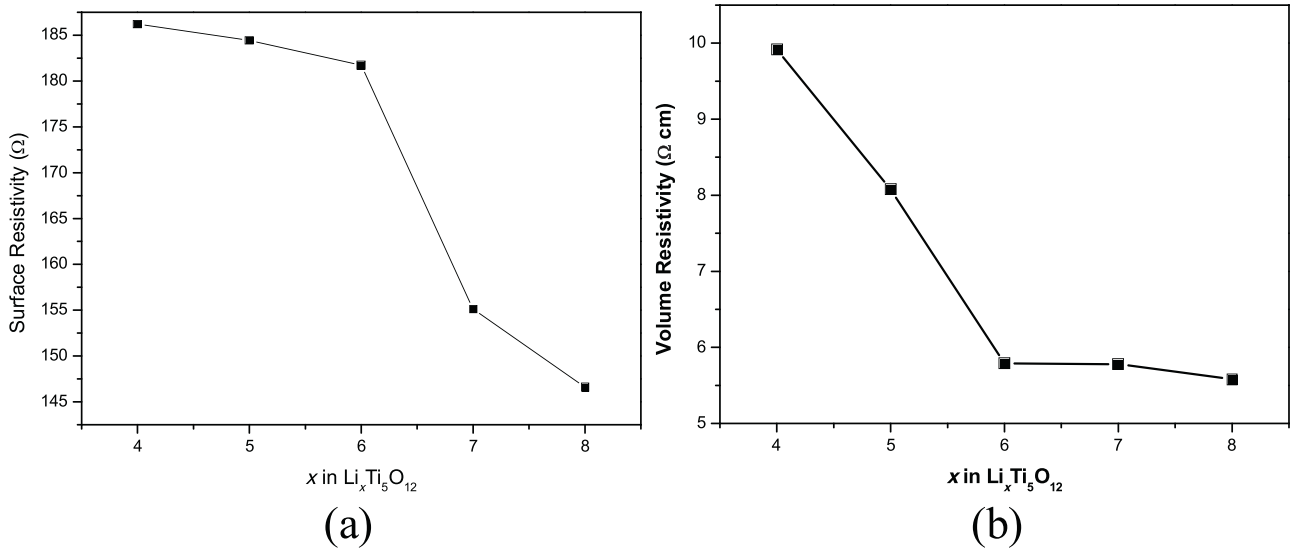

Fig. 2. (a) Surface and (b) volume resistivity of LTO-NF electrode at different states of lithiation.

Experimental method

Materials

Titanium(IV) butoxide, mesoporous carbon, anhydrous ethanol, lithium hydroxide monohydrate ($LiOH{\cdot}H_2O$), polyvinylidene fluoride (PVdF, $M_w \approx 534{,}000$), and *N*-methyl-2-pyrrolidone (NMP) were purchased from Sigma-Aldrich. Carbon black (Super-P) was purchased from Timcal. 1M $LiPF_6$ in ethylene carbonate (EC)/dimethyl carbonate (DMC) = 1/1 (v/v) was purchased from PANAX ETEC.

Synthesis of LTO nanoflakes

Typically, commercial LTO is produced via solid state reaction [16]; however, we employ a hydrothermal reaction in order to create nanoflake morphology, which has superior electrochemical properties which were explained in our previous research [13].

20 mmol of titanium butoxide was added to 40 mL of anhydrous ethanol and stirred. 16.8 mmol of $LiOH{\cdot}H_2O$ was added to 40 mL of deionized water and stirred until completely dissolved. The LiOH solution was added drop by drop to the titanium butoxide solution under vigorous stirring. The mixed solution was stirred for 1 h and transferred to a 100 mL Teflon-lined stainless steel autoclave and heated at 180 °C for 24 h. The product was centrifuged and washed with water twice and ethanol once and then dried in a vacuum oven overnight at 60 °C. The powder was then calcined at 600 °C for 6 h in air resulting in LTO-NF.

Material characterization

The surface morphology of the electrodes were characterized with field-emission scanning electron microscopy (FESEM, Hitachi S4800). Samples were prepared by opening cells in an argon-filled glovebox. The electrodes were dipped in dimethyl carbonate and vacuum dried at room temperature for 1 h. The electrodes were stored in glass vials inside the glove box and wrapped with paraffin film to prevent moisture from entering and causing unwanted reactions before SEM analysis.

Electrochemical characterization

A slurry was prepared by ball-milling at 300 rpm for 1 h. The slurry consisted of LTO-NF, MC, or a 1:1 wt.% mixture of LTO-NF and MC (80 wt.%) as the active material, carbon black (10 wt.%) as a conductive agent, and PVdF (10 wt.%) as a binder with NMP

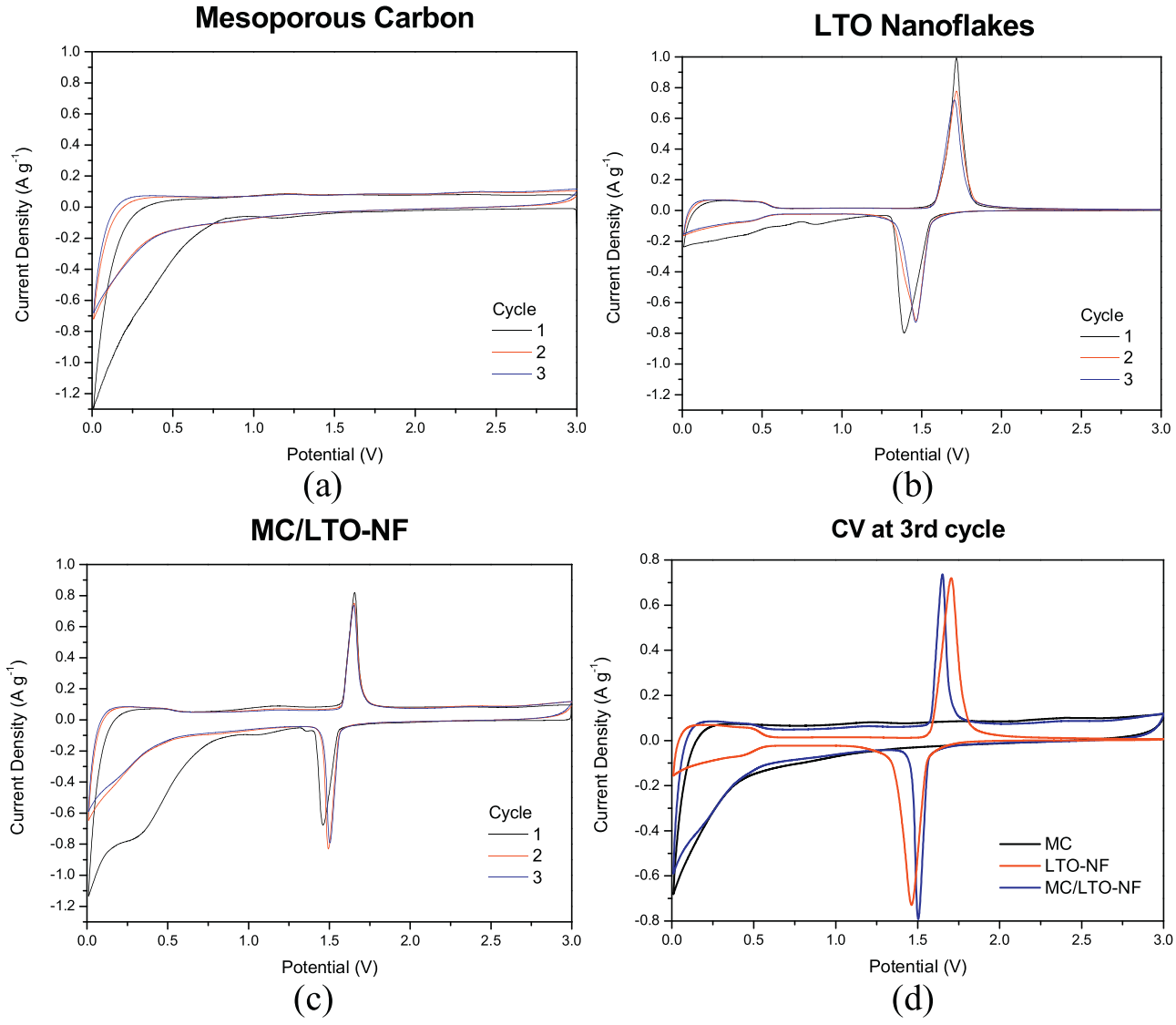

Fig. 3. Cyclic voltammograms of (a) MC, (b) LTO-NF, and (c) MC/LTO-NF for 3 cycles, and (d) the third cycle of all the electrodes at 0.2 mV s^{-1}.

added as a solvent to adjust the viscosity. The slurry was then coated onto a copper foil using a doctor blade apparatus and dried in a vacuum oven at 100 °C overnight. Then, working electrodes were cut into circular disks with a diameter of 14 mm. The electrodes had a mass loading of about 2 mg cm^{-2}. Coin cells were assembled in an argon-filled glovebox, with the working electrode, lithium metal as counter electrode, polyethylene separator, and 1 M $LiPF_6$ in EC/DMC = 1/1 (v/v) as electrolyte.

The coin cells were cycled at different current densities in a potential range of 0.01–3 V with a PEBC050.1 battery cycler (PNE SOLUTION). The rate capability of the cells were tested by charging and discharging at the same current densities of 0.05, 0.25, 0.5, 1, 2.5, 5, and back to 0.05 A g^{-1} for 10 cycles each. Cycle life was tested by charging and discharging at 175 mA g^{-1} for 100 cycles, then 500 mA g^{-1} for 500 cycles using the same cell. The cells were also characterized with cyclic voltammetry (CV) at scan rates of 0.2, 0.5, 1, 2, and 4 mV s^{-1} between the potential range of 0.01–3 V and electrochemical impedance spectroscopy (EIS) was conducted at a frequency range of 10 mHz–100 kHz with an amplitude of 10 mV using an AUTOLAB instrument (PGSTAT100, Eco Chemie).

Electron resistance of the LTO-NF electrodes at different states of lithiation were also measured using a 4-point probe CMT-SR1000 N Resistivity Measurement System (Advanced Instrument Technology). Electrodes were charged and discharged fully to determine the specific capacity for the $Li_7Ti_5O_{12}$ lithiated state which can be approximated at 1 V. The electrodes were removed from the coin cells at different states of lithiation which were based on the fraction of total specific capacity charged at the second cycle. The electrodes were then rinsed and prepared before resistivity measurements in the same way as described for the preparation of the electrodes for SEM analysis.

Results and discussion

Surface morphology

Fig. 1 shows the electrode surface morphology after 600 cycles. The formation of an SEI layer can clearly be seen when LTO-NF is discharged to 0.01 V in Fig. 1(b) compared to when it is discharged to 1 V in Fig. 1(a). Although the specific capacity of LTO is increased when discharged to 1 V, the SEI layer that is formed impedes the movement of Li^+ ions leading to reduced capacity at high charge and discharge rates. Fig. 1(c, d) shows the surface morphologies of MC and MC/LTO-NF composite, respectively. The MC/LTO-NF SEM

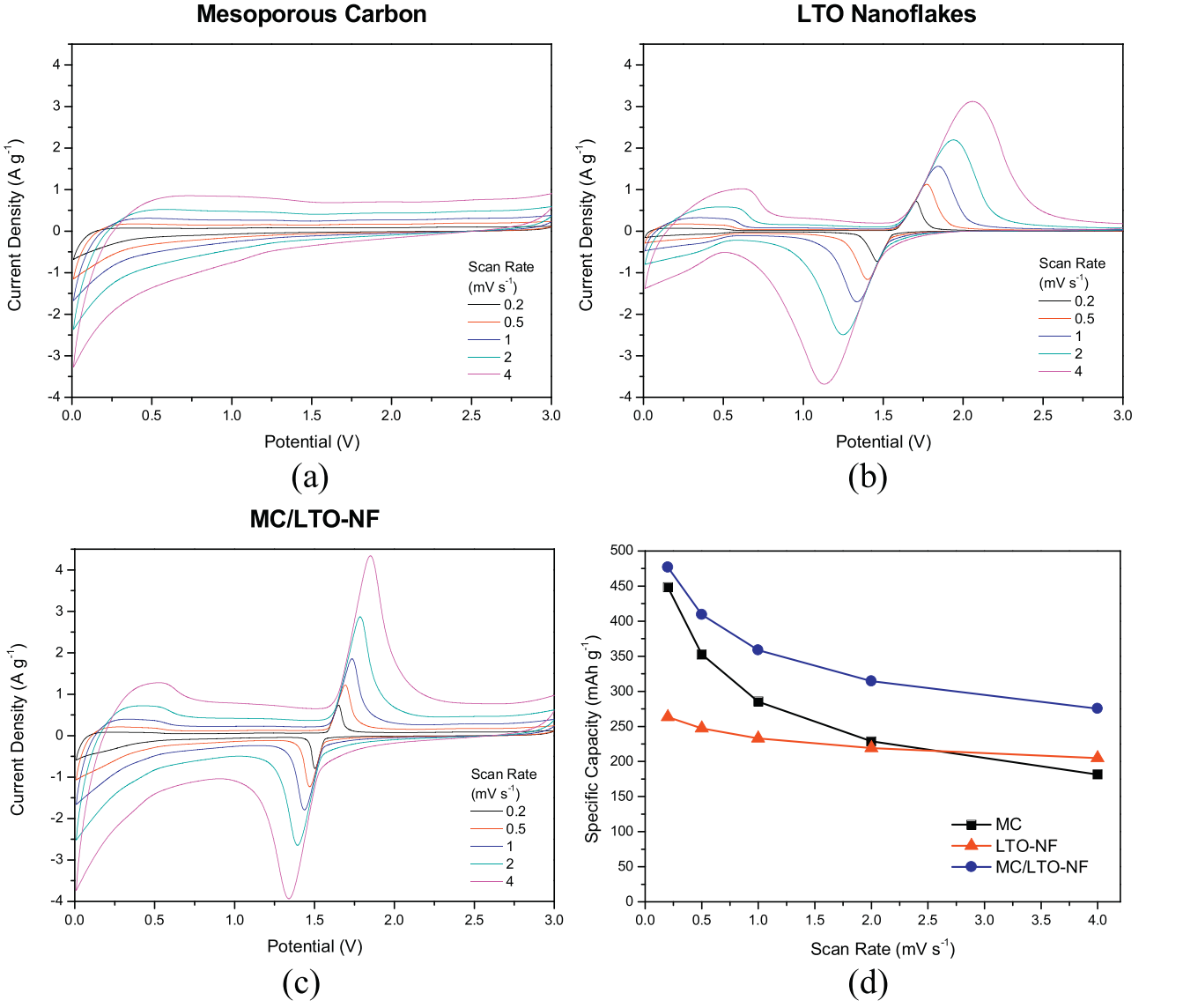

Fig. 4. Cyclic voltammograms at various scan rates of (a) MC, (b) LTO-NF, and (c) MC/LTO-NF, and (d) specific capacity as a function of scan rate for MC, LTO-NF, and MC/LTO-NF.

image shows that the MC and LTO-NF were well blended into a composite electrode.

Electronic resistance

As mentioned earlier, the electronic structure of LTO changes as it undergoes lithiation from insulating to metallic. In order to determine the effect of this change on the electron conductivity of the electrode, surface and volume resistivity was measured at various states of charge as shown in Fig. 2. It can be seen that before lithiation, $Li_4Ti_5O_{12}$ had a surface and volume resistivity of 186 Ω and 9.9 Ω cm^{-1}, respectively. With further lithiation, the surface and volume resistivities progressively drop as the LTO becomes more metallic in nature even when discharging below 1 V with a surface and volume resistivity of 147 Ω and 5.6 Ω cm^{-1} for $Li_8Ti_5O_{12}$. This demonstrates that LTO becomes more conductive as it becomes lithiated and that it can be used in conjunction with other anode materials that operate below 1 V.

Cyclic voltammetry

CVs of the electrodes are shown in Figs. 3 and 4 to analyze the electrochemical behavior of the composite material. Fig. 3(a–c) show the first three cycles at a scan rate of 0.2 mV s^{-1} for MC, LTO-NF, and MC/LTO-NF half cells. The first cycle shows the formation of the SEI layer at low voltages and the reversibility of the second and third cycles show that the SEI is highly stable. Fig. 3(a) ind a rectangular-shaped CV for the MC which indicates pseudocapacitive behavior with a lithium intercalation peak at low voltages similar to graphite. Fig. 3(b) shows the typical faradaic peaks of LTO at around 1.5 V corresponding with the change from $Li_4Ti_5O_{12}$ to $Li_7Ti_5O_{12}$ and a pseudocapacitive peak below 0.5 V corresponding with the change from $Li_7Ti_5O_{12}$ to $Li_{8.5+}Ti_5O_{12}$. Fig. 3(c) shows that MC/LTO exhibits both the pseudocapacitive behavior of MC as well as the faradaic peaks of LTO. A comparison of the third cycles of all the electrodes is also shown in Fig. 3(d) which displays that MC/LTO is able to maintain both the charge contribution from both MC and LTO although only half the mass of each component is used showing that the composite material has synergistic properties.

Fig. 4 shows the CVs of the electrodes at various scan rates to analyze electrochemical reversibility. The electrochemical reversibility of LTO-NF and MC/LTO-NF composite electrodes can be compared by looking at the difference in peak potentials (ΔE_p) and peak height (i_{pa}/i_{pc}) with ideal electrochemical reversibility when $\Delta E_p = 0$ and $i_{pa}/i_{pc} = 1$. The MC/LTO-NF composite electrode in Fig. 4(c) clearly shows a more reversible CV compared to the

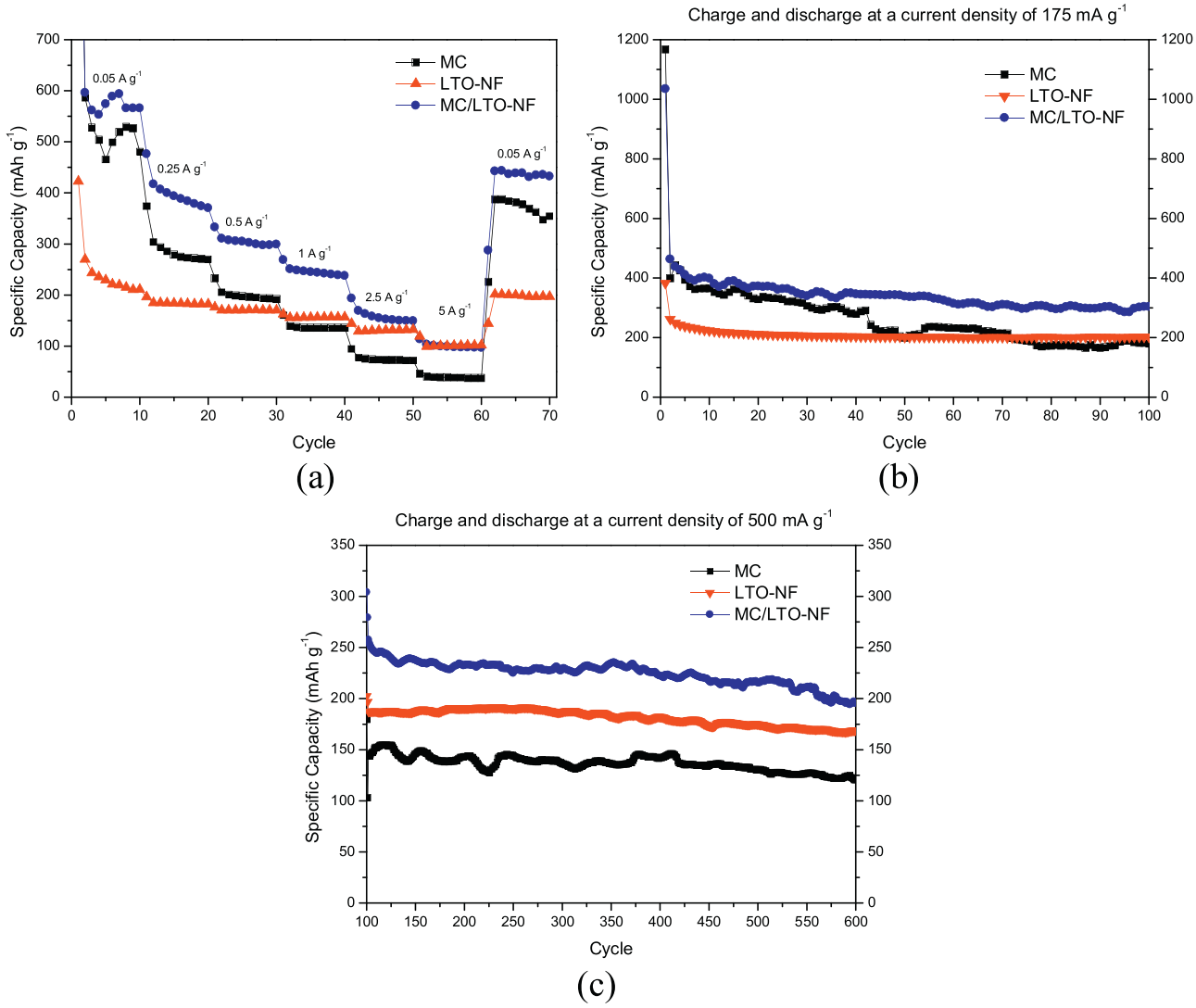

Fig. 5. Specific discharge capacity (a) at 0.05, 0.25, 0.5, 1, 2.5, and 5 A g^{-1} for 10 cycles each, (b) 100 cycles at a charge and discharge current density of 175 mA g^{-1}, and (c) 500 cycles at a charge and discharge current density of 500 mA g^{-1}.

LTO-NF electrode in Fig. 4(b) with $\Delta E_p = 0.51$ and $i_{pa}/i_{pc} = 1.1$ compared to $\Delta E_p = 0.92$ and $i_{pa}/i_{pc} = 0.85$, respectively, at a scan rate of 4 mV s^{-1}. This shows that the electron transfer kinetics as well as Li^+ ion diffusion is enhanced for the MC/LTO-NF composite electrode. The CV also shows that the peaks for MC/LTO-NF are also sharper and narrower which also suggests increased charge transfer kinetics.

Galvanostatic charge–discharge

The various electrode materials were tested for rate capability and cycle performance as shown in Fig. 5. The cells were discharged to 0.01 V to increase the specific capacity and energy density of the anode materials. Fig. 5(a) shows the specific capacity at various current densities, and the specific capacity of MC/LTO-NF exceeds that of MC and LTO-NF up to a current density of 5 A g^{-1}. Because the MC/LTO-NF composite is a 1:1 wt.% of MC and LTO-NF, the expected result is that the specific capacity would be the average of the two materials, but the experimental results show that there is a synergistic behavior between the two materials which enhances the electrochemical performance of the composite which causes higher specific capacity. This is due to the conductive nature of LTO as it is lithiated below 1 V.

Based on the rate performance test, the cells were cycled at current densities of 175 mA g^{-1} and 500 mA g^{-1} for 100 and then 500 cycles, consecutively, as shown in Fig. 5(b, c). The MC and MC/LTO-NF composite electrodes show a high initial discharge specific capacity of above 1000 mA h g^{-1} which drops quickly after the first cycle due to the formation of the SEI layer. The MC/LTO-NF composite electrode started to stabilize after 100 cycles ending with a specific capacity of 300 mA g^{-1}. The cells were also cycled at a high current density of 500 mA g^{-1}. The MC performed relatively poorly compared to bare LTO-NF; however, the MC/LTO-NF composite was still able to achieve higher specific capacity over 500 cycles. These results show the potential for this material to be used in real world applications.

Electrochemical impedance spectroscopy

Fig. 6 shows the Nyquist plots of the electrode materials after the cycle tests. The inset shows the semicircles in more detail from which the resistance due to SEI (R_{SEI}), and charge transfer resistance (R_{ct}) can be determined. EIS starts from the high frequency region on the left side to the low frequency region on the right. The size of the first small semicircle at the highest frequencies corresponds with the R_{SEI}. The Nyquist plot shows

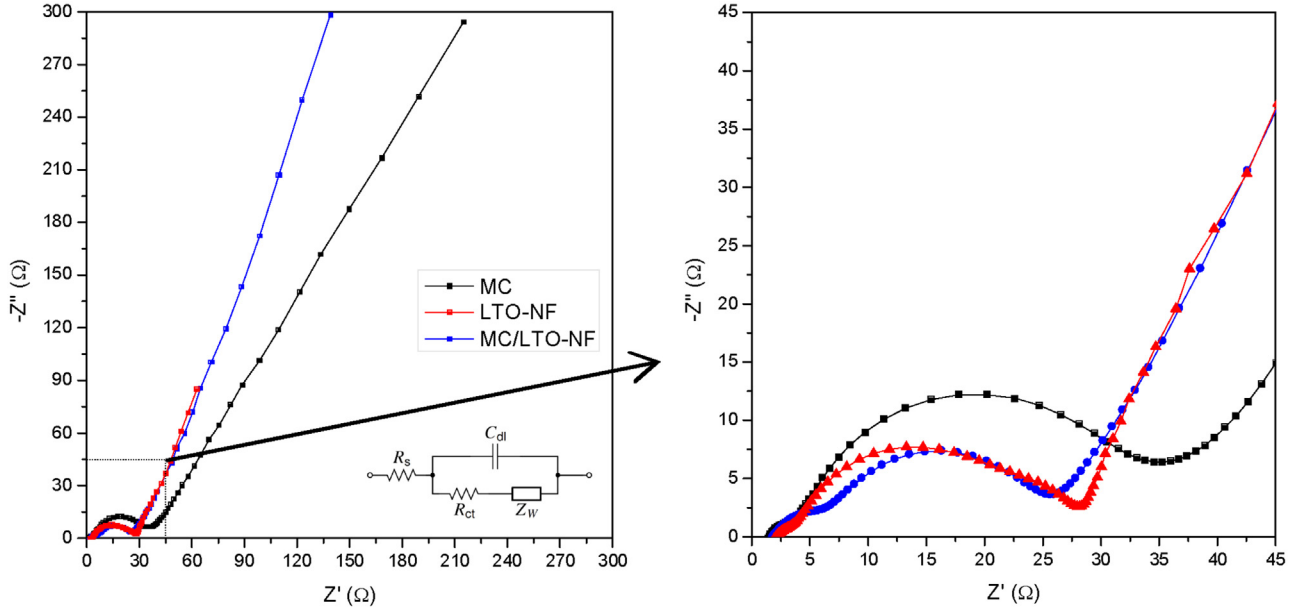

Fig. 6. Electrochemical impedance spectroscopy after cycling.

Table 1
Comparison of other research on LTO discharged to 0.01 V with our work.

Year	Anode material	Capacity (mAh g^{-1})	Cycles	Discharge rate (mA g^{-1})	References
2008	$Li_4Ti_5O_{12}$	200	3	0.2 mA cm^{-2}	[17]
2008	$Li_4Ti_5O_{12}$	195	90	175	[18]
		188	120	525	
2015	$Li_4Ti_5O_{12}/Al_2O_3$	175	40	200	[19]
		145	50	400	
2015	$Li_4Ti_5O_{12}/Co_3O_4$	300	50	160	[20]
		300	10	320	
2016	$Li_4Ti_5O_{12}$	200	100	175	[21]
		120	300	875	
2017	$Li_4Ti_5O_{12}/TiO_2$	170	100	175	[22]
		165	40	350	
2019	$Li_4Ti_5O_{12}$	225	150	20	[23]
2019	$Li_4Ti_5O_{12}$/MC	300	100	175	Our work
		200	600	500	

that the MC/LTO-NF composite has a R_{SEI} of 4.0 Ω which is higher the then 1.3 Ω for LTO-NF, which is due to the increased SEI formation as seen from the larger drop is specific capacity from first to second cycle in Fig. 5(b). However, the R_{ct} for MC/LTO-NF was 19.3 Ω compared to 24.7 Ω for LTO-NF, which shows enhanced charge transfer kinetics for MC/LTO-NF. The low frequency region can also be used to interpret the Warburg impedance with a more vertical tail corresponding with improved mass transfer. The LTO-NF and MC/LTO-NF composite had a more vertical tail compared to the MC which denotes improved Li^+ ion diffusion through the electrode material. Thus, the addition of LTO-NF to MC as a composite material was able to improve the electrochemical performance by improving charge and mass transfer kinetics.

Conclusion

LTO is not typically discharged to 0.01 V although it results in higher specific capacity and energy density due to the formation of an SEI layer leading to a decrease in performance for high power applications. However, when used in conjunction with another anode material to form a composite, it can exhibit synergistic behavior depending on the anode material to increase its electrochemical performance. The reason for the synergistic action of LTO is explained by the change in its electronic structure allowing it become more conductive and metallic in nature as it undergoes lithiation. In this research, LTO-NF has been used rather than LTO nanoparticles and this is highly recommended because of the superior electrochemical properties of LTO-NF which we have shown in previous research [8]. Our research has been compared with other research where LTO and LTO composite anodes have been discharged to 0.01 V as shown in Table 1. We were able to achieve higher specific capacity at various current densities and our results show that the MC/LTO-NF composite has real world applications as an energy storage device. Furthermore, our research shows that LTO has good synergistic properties as a composite anode material. This possibility has not yet been extensively researched and we believe that there is still a lot of room for growth for increasing the energy and power density using LTO composites.

Acknowledgements

This research was supported by a R&D grant (20001114) from the Korean Ministry of Trade, Industry & Energy.

References

[1] C.P. Sandhya, B. John, C. Gouri, Ionics 20 (2014)601620.
[2] T. Ohzuku, A. Ueda, N. Yamamoto, J. Electrochem. Soc. 142 (1995) 1431.
[3] K. Mukai, Y. Kato, H. Nakano, J. Phys. Chem. C. 118 (2014) 2992.
[4] S. Wang, K. Yang, F. Gao, D. Wang, C. Shen, RSC Adv. 6 (2016) 77105.
[5] Z. Zhong, C. Ouyang, S. Shi, M. Lei, ChemPhysChem 9 (2008) 2104.
[6] W.J.H. Borghols, M. Wagemaker, U. Lafont, E.M. Kelder, F.M. Mulder, J. Am. Chem. Soc. 131 (2009) 17786.
[7] C.Y. Ouyang, Z.Y. Zhong, M.S. Lei, Electrochem. Comm. 9 (2007) 1107.
[8] G. Wang, R. Liu, M. Chen, H. Kang, X. Li, K. Yan, Korean J. Chem. Eng. 29 (2012) 1094.
[9] J.-H. Kim, M.-J. Jung, M.-J. Kim, Y.-S. Lee, J. Ind. Eng. Chem. 61 (2018) 368.
[10] G.-H. An, H. Kim, H.-J. Ahn, J. Ind. Eng. Chem. 68 (2018) 146.
[11] J. Wang, J.-Y. Li, Z.-B. Shao, H.-T. Fan, H.-Q. Ru, S.-Y. Zang, Korean J. Chem. Eng. 36 (2019) 281.
[12] S. Ghosh, W.D. Yong, E.M. Jin, S.R. Polaki, S.M. Jeong, H. Jun, Korean J. Chem. Eng. 36 (2019) 312.
[13] C.Y. Bon, P. Isheunesu, S. Kim, M. Mwemezi, Y.I. Kim, Y.J. Lee, J.M. Ko, Energy Technol. 6 (2019) 2461.
[14] H. Xu, J. Chen, Y. Li, X. Guo, Y. Shen, D. Wang, Y. Zhang, Z. Wang, Sci. Rep. 7 (2017) 2960.
[15] L. Wu, X. Leng, Y. Liu, S. Wei, C. Li, G. Wang, J. Lian, Q. Jiang, A. Nie, T.-Y. Zhang, ACS Appl. Mater. Interfaces 9 (2017) 4649.
[16] S.H. Kim, H. Park, S.H. Jee, H.S. Ahn, D.-J. Kim, J.W. Choi, S.J. Yoon, Y.S. Yoon, Korean J. Chem. Eng. 26 (2009) 485.
[17] X.L. Yao, S. Xie, H.Q. Nian, C.H. Chen, J. Alloys Compd. 465 (2008) 375.
[18] H. Ge, N. Li, D. Li, C. Dai, D. Wang, Electrochem. Commun. 10 (2008) 719.
[19] D. Ahn, X. Xiao, Front. Energy Res. 3 (21) (2015) 1.
[20] J.-E. Hong, R.-G. Oh, K.-S. Ryu, J. Electrochem. Soc. 162 (2015) A1978.
[21] C. Han, Y.-B. He, S. Wang, C. Wang, H. Du, X. Qin, Z. Lin, B. Li, F. Kang, ACS Appl. Mater. Interfaces 8 (2016) 18788.
[22] M. Ding, H. Liu, X. Zhao, L. Pang, L. Deng, M. Li, RSC Adv. 7 (2017) 43894.
[23] H. Liu, Z. Zhu, J. Huang, X. He, Y. Chen, R. Zhang, R. Lin, Y. Li, S. Yu, X. Xing, Q. Yan, X. Li, M.J. Frost, K. An, J. Feng, R. Kostecki, H. Xin, S.P. Ong, P. Liu, ACS Mater. Lett. 1 (2019) 96.